Journal of Building Performance Simulation

ISSN: (Print) (Online) Journal homepage: https://www.tandfonline.com/loi/tbps20

Risk-informed multi-criteria decision framework for resilience, sustainability and energy analysis of reinforced concrete buildings

Esmaeel Asadi , Zhenglai Shen , Hongyu Zhou , Abdullahi Salman & Yue Li

To cite this article: Esmaeel Asadi , Zhenglai Shen , Hongyu Zhou , Abdullahi Salman & Yue Li (2020) Risk-informed multi-criteria decision framework for resilience, sustainability and energy analysis of reinforced concrete buildings, Journal of Building Performance Simulation, 13:6, 804-823, DOI: 10.1080/19401493.2020.1824016

To link to this article: https://doi.org/10.1080/19401493.2020.1824016

Published online: 04 Oct 2020.

JOURNAL OF BUILDING PERFORMANCE SIMULATION
2020, VOL. 13, NO. 6, 804–823
https://doi.org/10.1080/19401493.2020.1824016

Risk-informed multi-criteria decision framework for resilience, sustainability and energy analysis of reinforced concrete buildings

Esmaeel Asadi [a], Zhenglai Shen [b], Hongyu Zhou [b], Abdullahi Salman [c] and Yue Li [d]

[a]College of Architecture & Environmental Design, Kent State University, Kent, OH, USA; [b]Department of Civil and Environmental Engineering, The University of Tennessee, Knoxville, TN, USA; [c]Department of Civil and Environmental Engineering, The University of Alabama in Huntsville, Huntsville, AL, USA; [d]Department of Civil Engineering, Case Western Reserve University, Cleveland, OH, USA

ABSTRACT

With recent advancement in energy-based sustainable design of building structures, the need for inclusive yet practical models to integrate resilience and sustainability is increasingly recognized. This paper integrates structural seismic resilience and sustainability assessment methods with whole-building energy simulation techniques to present a new comprehensive decision model for the design of buildings. Risk-based multi-attribute utility theory and analytic hierarchy process are used to develop a multi-criteria decision-making (MCDM) framework considering various economic, social and environmental criteria involved in design of buildings. The model is implemented on a number of RC buildings, and the influence of building configuration on environment, seismic performance, and energy consumption is studied. It is found that shear wall ratio plays a significant role in both seismic loss and energy consumption of RC buildings. Increasing the shear wall ratio effectively reduces the direct monetary loss and downtime as well as energy consumption.

ARTICLE HISTORY
Received 4 September 2019
Accepted 10 September 2020

KEYWORDS
Risk-informed multi-criteria decision-making; life cycle cost; energy simulation; sustainability; resilience; RC buildings

Introduction

Mounting evidence of human-induced climate change and increasing loss due to various natural hazards have reinforced experts' efforts to develop new tools and techniques for sustainable and resilient design and construction of civil infrastructure. To reduce carbon footprint and other environmental impacts, several studies aimed to include sustainability criteria in the design of various structure and infrastructure systems (Kamali, Hewage, and Milani 2018; Nadoushani et al. 2017; Padgett and Li 2016). Natural hazards, especially earthquakes, cause billions of dollars of economic loss and claim thousands of lives every year. In recent decades, seismic risk has increased due to significant population/industry growth in earthquake-prone urban regions and increasing vulnerability of aging infrastructure (FEMA, Pacific Disaster Center, and USGS 2017). To mitigate environmental impacts while addressing the increasing risk due to seismic hazard, this paper aims to present a comprehensive decision-making framework, which integrates resilience, sustainability, and energy criteria for building design.

Resilience is the capability of a building to resist, adapt to and recover from a disruptive event such as an earthquake. The seismic resilience of buildings and other structures has been extensively studied in recent years (Bocchini et al. 2014; Roostaie, Nawari, and Kibert 2019; Asadi, Li, and YeongAe 2018; Bruneau et al. 2003). In 2012, FEMA published the FEMA P-58 report providing a uniform approach for estimating key seismic resilience metrics, namely repair/replacement cost, downtime and the number of casualties (Belleri and Marini 2016; FEMA 2012). In this paper, these metrics are used to evaluate the resilience of a building.

The building sector is also one of the main consumers of energy in the USA, accounting for over 40% of total energy consumption and producing about 38% of greenhouse gas (GHG) emissions in the US (Belleri and Marini 2016; Basbagill et al. 2013; CMU GDI 2018; Junnila, Horvath, and Guggemos 2006). About 30% of all the energy consumed in a building during its lifespan is in the form of embodied energy (Ibn-Mohammed et al. 2013). In addition to embodied energy, buildings consume substantial operational energy for indoor environment conditioning (heating, cooling, ventilation), powering equipment, lighting, etc., over their life cycle. Increasingly, whole-building energy simulation is being conducted to achieve energy-efficient and sustainable designs. Yet, to achieve a holistic design framework, sustainability needs to be studied considering its interrelation and overlaps with

CONTACT Esmaeel Asadi easadi@kent.edu

resilience (Belleri and Marini 2016; Asadi, Salman, and Li 2019; Park, Hwang, and Oh 2018).

Sustainability is defined as a function of environmental, economic and social impacts of building's construction and maintenance, and demolition. Economic metrics such as construction and maintenance costs and environmental metrics such as carbon footprint have been used to measure sustainability (Roostaie, Nawari, and Kibert 2019; Kamali, Hewage, and Milani 2018). Life cycle analysis is commonly used to find the sustainability metrics of a building. To quantify the total life cycle cost, a simple approach used in the literature is to convert all losses, including environmental, life and time losses, into a monetary loss (Han, Li, and van de Lindt 2016; Mitrani-Reiser 2007). This approach, however, adds to uncertainty because of regional and case-based assumptions required for such conversion (Lloyd and Ries 2007; Chau, Leung, and Ng 2015). Given the uncertainties, adding all converted losses together may yield inaccurate conclusions. Another approach is multi-criteria decision models (MCDM) where the sustainability and resilience metrics, criteria or attributes are kept in its original unit/space. MCDM provides more flexibility for problems where the objective is not solely minimizing monetary losses. Multi-criteria decision analysis has been used in the architectural design and construction industry (Baglivo, Congedo, and Fazio 2014; Hopfe, Augenbroe, and Hensen 2013; Invidiata, Lavagna, and Ghisi 2018; Kokaraki et al. 2019). Baglivo, Congedo, and Fazio (2014) used MCDM to find the optimal wall configuration based on sustainability factors such as thermal performance, operational energy use, embodied energy, productivity and construction cost. Hopfe, Augenbroe, and Hensen (2013) also used analytic hierarchy process (AHP) for building energy performance assessment considering the energy use, acoustical and thermal-comfort performance, and indoor air quality. However, they all focus on architectural criteria leaving out structural performance, resilience against natural hazards, and environmental consequence of construction and maintenance. Few studies used MCDM for building design based on both resilience and sustainability criteria (Kokaraki et al. 2019).

This paper integrates resilience, sustainability and energy analysis methodologies for buildings and presents a new comprehensive trilateral decision-making framework for their design. The proposed trilateral model uses both AHP and risk-based multi-attribute utility theory (MAUT) to include various resilience, sustainability and energy criteria in decision analysis. A survey is conducted to quantify the importance factor for each criterion considering seven different scenarios/objectives. Criteria quantified for seismic resilience include asset loss, time loss, number of casualties and fatalities. For sustainability, life-cycle construction and maintenance costs and GHG emission are studied. Using whole-building energy simulation, annual energy consumption, cost, and associated GHG emission are studied as well. The framework is implemented for two groups of commercial reinforced concrete (RC) buildings located in Los Angeles (LA), CA and Boston, MA.

Proposed multi-criteria decision-making framework

The proposed decision-making framework consists of three main modules: (1) System Concept and Criteria (SCC) Module, (2) Resilience, Sustainability, and Energy Analysis (RSEA) Module, (3) Multi-Criteria Decision Making (MCDM) Module. Figure 1 depicts its main components and their inter-connections. The model consists of a feedback loop to update decisions based on new data obtained from monitoring and inspection, or due to change in hazard, vulnerability or loss parameters. Monitoring and inspection through a feedback loop are not studied here.

System concept and criteria (SCC) module

The project objectives, system properties, and analysis and design specifications and assumptions will be defined in the SCC module. Similarly, the scope of assessment and the importance of each metric over others (e.g. monetary loss importance over GHG emission) are defined in this module according to decision-maker's preference and the objectives of the project. The output of this module is the archetype models ready for loss, life cycle and energy-consumption analyses. The models include all structural and non-structural components of the building for component-level resilience and sustainability assessment and the thermal zone arrangement, material properties for walls, roof, façade, etc., and HVAC, lighting and shading components for whole-building energy simulation. More details on SCC module are presented in Asadi, Salman, and Li (2019) and Asadi (2020). Numerical models developed in SCC module go to RSEA module where they are analysed for various criteria depending on project requirements.

Resilience, sustainability and energy analysis (RSEA) module

The integrated core module, RSEA, consists of three submodules where resilience, sustainability and whole-building energy criteria are quantified. Figure 2 shows the stepwise illustrative procedure for the RSEA module.

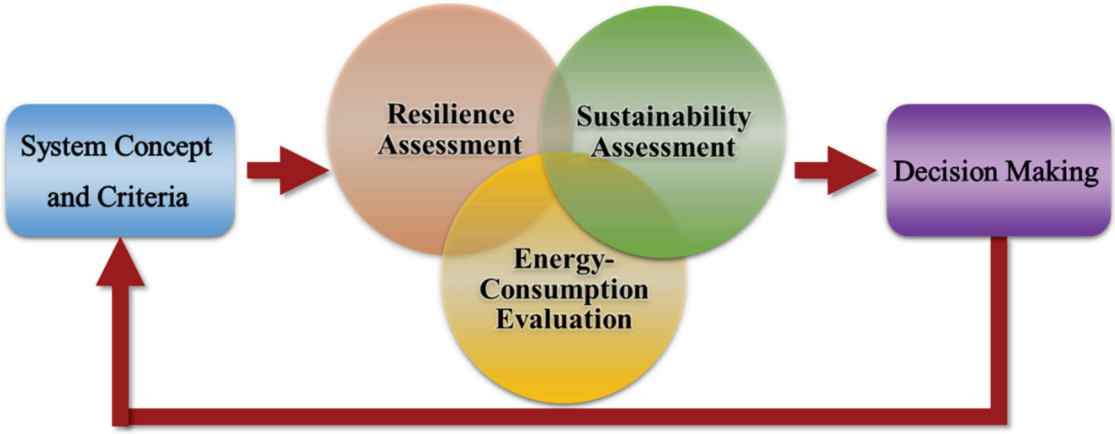

Figure 1. Main components of the proposed framework.

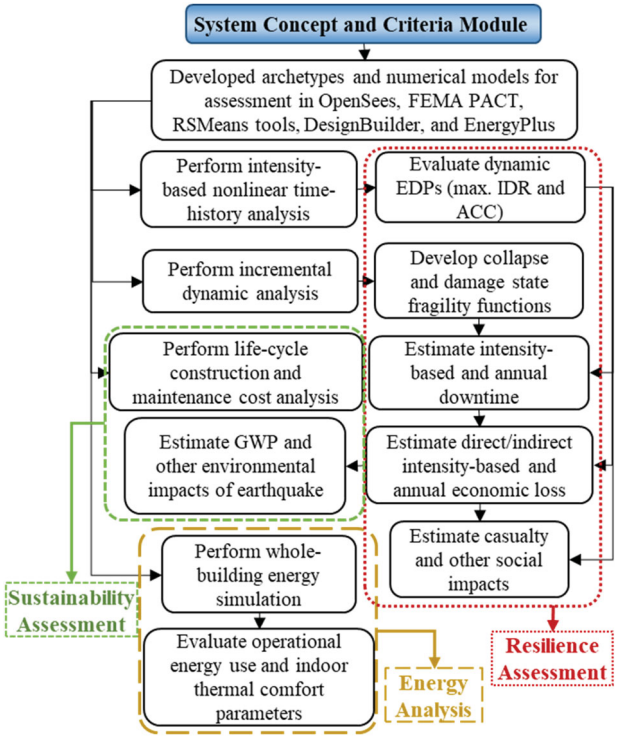

Figure 2. Seismic resilience, sustainability and energy-consumption analysis (RSEA) module.

Collapse fragility analysis and time-history dynamic analysis results are used as inputs for seismic loss analysis, while the outputs of seismic repair cost, construction and maintenance costs are used to evaluate GHG emissions. The simulation models are analysed, and the outputs are transferred to the MCDM module where decision analysis is performed.

Resilience assessment

Resilience (R) can be quantified as the integration of functionality (Q) over a time interval (T_R) after the occurrence of an event at time t_0 (Cimellaro, Reinhorn, and Bruneau 2010):

$$R = 1/T_R \int_{t_0}^{t_0+T_R} Q(t)\mathrm{d}t \tag{1}$$

$$Q(t) = (1 - L_t) \times f_R \tag{2}$$

where L_t is the whole-building loss function and f_R is the recovery function. Loss is the key parameter in the above formula embodying earthquake consequences. For mutually exclusive seismic events, the total probability of seismic loss at a given earthquake intensity is defined in the following (Belleri and Marini 2016; Ramirez and Miranda 2012).

$$\mathrm{P}(L > l_i|IM = z) = \int_{\mathrm{EDP}} \int_{\mathrm{DS}} \mathrm{P}(L > l_i|\mathrm{DS} = \mathrm{DS_{ij}}) \mathrm{P}(\mathrm{DS}|\mathrm{EDP} = d)\mathrm{P}(\mathrm{EDP}|\mathrm{IM} = z)\mathrm{dDS}\,\mathrm{dEDP} \tag{3}$$

where $\mathrm{P}(L > l_i|IM = z)$ is the probability of having a loss greater than l_i given that hazard intensity is equal to z, $\mathrm{P}(L > l_i|\mathrm{DS} = \mathrm{DS_{ij}})$ is the probability of having a total loss greater than l_i given that damage state of DS_i is achieved for component j, $\mathrm{P}(DS|EDP = d)$ is the probability density function (PDF) of achieving a damage state given that the engineering demand parameter (EDP) reaches a certain value of d, and $\mathrm{P}(EDP|IM = z)$ is the PDF of the EDP conditioned on a certain hazard intensity, z. For component-level loss estimation, the conditional consequence function, $\mathrm{P}(L > l_i|DS = DS_{ij})$, requires a database of repair cost/time and other consequence functions for every component, which is provided with FEMA P-58 in FEMA PACT (FEMA 2012). The fragility functions obtained from nonlinear dynamic analysis are used to find the probability of reaching a certain damage state for each damageable component.

For time-based loss estimation, the annual probability of loss, $\mathrm{P}(L > l_i)$, given the annual probability of each

earthquake intensity, $P(IM = z)$, will be

$$P(L > l_i) = \int_{IM} P(L > l_i | IM = z) P(IM = z) dIM \quad (4)$$

The loss (L), in equations above, may be any kind of loss due to any stochastic hazard including monetary, time, life or environmental loss due to earthquake.

Sustainability assessment

Sustainability involves a broad range of metrics, but it is commonly quantified using three main measures: environmental, economic and social consequences of the product or process. Some criteria are both a resilience and sustainability measure and some are both a sustainability and energy measure. Considering this inter-relationship, these consequences can be incorporated through quantitative parameters such as embodied energy, operational energy use, construction and maintenance costs, and economic loss, downtime, and casualties due to natural or manmade hazards.

The initial cost of the buildings was analysed using data-based life cycle cost estimator tools considering the construction cost of all structural and non-structural components of a building. Particularly, RSMeans Data Online (2018) was used to estimate the construction cost including substructure cost, shell cost, interiors cost, services cost, and contractor and architectural fees. The tasks and periodicities recommended by Whitestone cost reference (Abate et al. 2009) are used for estimating building maintenance cost. The Whitestone database was used for estimating ecological footprint due to the operation and maintenance of residential buildings as well (Basbagill et al. 2013; Martínez-Rocamora, Solís-Guzmán, and Marrero 2017).

Maintenance and energy costs and benefits need to be discounted to a present value. The net present value of a future cost $C(t)$ at the year t can be calculated as (Zheng and Lai 2018)

$$C(t) = \sum_{t=1}^{n} \frac{B_t - M_t}{(1+r)^t} \quad (5)$$

where r, B_t, M_t and n are the annual monetary discount rate, the monetary benefit gained, maintenance cost and the number of years considered.

All construction, operation, maintenance activities have environmental impacts and need to be considered in an MCDM framework. Based on the theorem of total probability, the sustainability function (M_S) can be expressed as a function of conditional consequence functions as follows (Belleri and Marini 2016; Ellingwood 2005):

$$M_S = \int_{IM} \int_{EDP} \int_{DS} C_{Cons|DS}(t) P_{DS|EDP}(t) P_{EDP|IM}(t) P_{IM}(t) dDS\, dEDP\, dIM \quad (6)$$

where $C_{Cons|DS}(t)$, $P_{DS|EDP}(t)$, $P_{EDP|IM}(t)$ and $P_{IM}(t)$ are the conditional consequence given a damage state, the conditional probability of a damage state given the EDP, the conditional probability of an EDP given a hazard intensity and the annual mean rate of occurrence of hazard IM, all at time t, respectively. The consequence functions, $C_{Cons|DS}$, are evaluated using the economic input-output life-cycle analysis (EIO-LCA) model presented by Carnegie Mellon University (CMU GDI 2018). The EIO-LCA uses both environmental and historical economic data aiming to answer shortcomings of process-based LCA such as requiring heavy data, being time-consuming and expensive, and selecting proper system boundaries. EIO-LCA method provides more flexibility since it can effortlessly be used along with related studies in economics and insurance industry. EIO-LCA calculates the environmental consequences of the building construction, maintenance and seismic repair using their corresponding cost. It considers both the direct impacts of the product/project and the indirect impacts in the supply chain (Ochoa, Hendrickson, and Scott Matthews 2002).

Energy consumption and cost analysis

The whole-building energy analysis is performed in widely used EnergyPlus (ASHRAE 2016a; Invidiata, Lavagna, and Ghisi 2018; Robati, Kokogiannakis, and McCarthy 2017). Through concurrently solving the heat balance equations of thermal zones and plant systems of the building, EnergyPlus calculates energy consumption for indoor heating and cooling, water heating, ventilation, lighting, and plug and process loads (Crawley et al. 2001). EnergyPlus considers both source and site energy consumption in various units including kWh. The source energy is the energy used to generate the electricity, e.g. natural gas or coal, which has a significant impact on the GHG emissions due to energy consumption. The site energy is the energy consumed in the building in the form of electricity or natural gas. To estimate the current cost of energy, the yearly average price data is collected from US BLS (2018) and future cost is discounted using Equation (5). National Institute of Standards and Technology (NIST) also provides the projected energy price indices and discount factors for life cycle cost (LCC) analysis which is used to verify the cost estimation (Lavappa and Kneifel 2018).

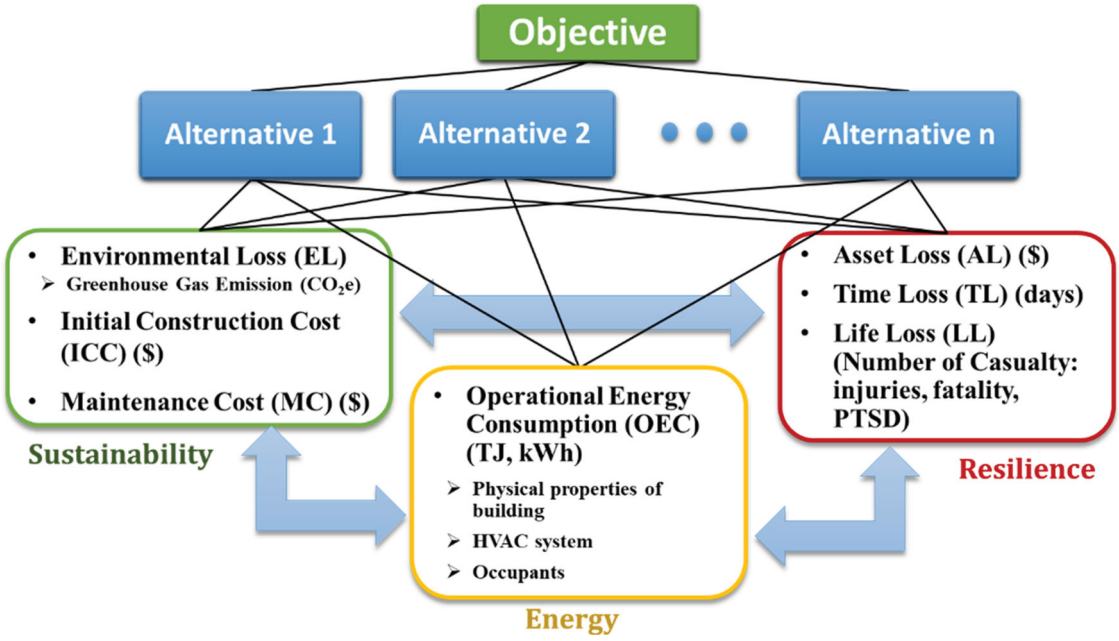

Figure 3. Analytic hierarchy model considered for decision analysis and the trilateral sets of criteria/attributes.

Multi-criteria decision-making module

Trilateral criteria/attributes

Attributes are various dimensions or properties of the applied system from which the alternatives can be viewed and compared (Triantaphyllou et al. 1998). The effective metrics/criteria are categorized into three sets, i.e. resilience, sustainability and energy, to match the RSEA module outputs creating a trilateral decision analysis framework. Figure 3 depicts the three-level AHP model used and categorizes the trilateral sets of criteria considered. The AHP shows the relationship between the objectives of the project, the criteria and the alternatives the decision-maker has (Mateo and Cristóbal 2012). The elements of each level need to be compared to each other from bottom to top to achieve the AHP-based goal. At the lowest level, the criteria are to be compared to each other to create pairwise comparison matrices. These matrices are used to find the importance/weight factors for each criterion compared to others. These factors are then used to evaluate the utility functions, as described in the next section.

The set of resilience metrics incorporate three criteria which are asset, time, and life losses due to the hazard, here earthquake hazard. The seismic asset loss (AL) measured in US Dollars may include all direct and indirect monetary losses such as repair/replacement cost, closure cost and relocation cost due to earthquake. The time loss (TL), commonly measured in number of days, is the time it takes for the building to return to its original functionality after an extreme event. Depending on the system being studied, it may also be referred to as restoration or recovery time or downtime. The life loss (LL) represents the social impacts of earthquake and is commonly measured in terms of number of casualties, injuries, fatalities, and if data is available number of Post-Traumatic Stress Disorder (PTSD) cases and displaced households.

Sustainability involves social, economic and environmental metrics. Given its overlap with resilience in this study, the emphasis for the sustainability submodule is on the environmental consequence and construction and maintenance costs. A component-level approach is recommended for Initial Construction Cost (ICC) evaluation where the replacement cost of all structural, non-structural and utility components of the building is included. ICC is also evaluated in US dollars. Cost of repairing and maintaining interior finishes, exterior closure, plumbing, conveying, fire and electrical equipment, etc. due to aging is also an economic criterion of sustainability. Here, maintenance costs are evaluated in US dollars for a 50-year lifespan, abbreviated MC.

Moreover, an environmental loss (EL) due to construction, operation, maintenance and seismic repair/replacement is considered. EL can be measured in terms of ton CO_2 equivalent GHG emission, m^3 or kGal water withdrawal, ton waste or pollution produced, etc. depending on the project requirement and/or decision maker's preference.

The third set of criteria includes energy-consumption metrics such as annual operational energy consumption in kWh or annual operational energy cost (OEC) in US dollars. These metrics depend on construction materials, glazing type, wall thickness, HVAC specification,

age of the building, number of occupants and maintenance/repair plan. These metrics are evaluated through whole-building simulation.

In practice, all or some of the mentioned metrics may be included in the decision analysis. The stakeholder or the decision-maker may specify which metric needs to be considered depending on the available data and project specifications and objectives. In the case studies presented in this paper, seismic repair/replacement costs and time, the number of fatality and injuries due to earthquakes, initial construction cost, maintenance costs, annual operational energy cost, and environmental impacts (GHG emission) due to construction, operation, maintenance and seismic repair/replacement are included in the decision-making process.

Multiple attribute decision making

In MAUT, utility functions measuring the preference over a set of attribute need to be defined for each alternative and each attribute. Utility takes a value of 0 (for the worst outcome) to 1 (for the best outcome). To achieve a risk-informed decision, the utility can be defined with three attitudes towards risk: risk aversion, risk-neutral (linear), and risk-seeking. For risk-neutral attitude, the utility function (u_{ij}) can be found as follows for a minimization criterion:

$$u_{ij(x)} = \frac{A_{max,i} - x_{ij}}{A_{max,i} - A_{min,i}} \tag{7}$$

where x_{ij} is the score (resilience, sustainability, or energy metric) for criterion/attribute i ($i = 1, \ldots, n$) and alternative j ($j = 1, \ldots, m$). $A_{max,i}$ and $A_{min,i}$ are the maximum and minimum scores evaluated for each i attribute among all m alternatives, respectively. For risk aversion and seeking utility functions an exponential equation is used (Wood and Khosravanian 2015; Ellingwood and Lee 2016; Lee, Burton, and Lallemant 2018):

$$u_{ij(x)} = \frac{1 - \exp(-r \times x_{ij})}{1 - \exp(-r)} \tag{8}$$

where r is a non-zero risk aversion factor. Positive values for r give convex functions (risk aversion) and negative r values give concave functions (risk seeking), as depicted in Figure 4.

As described, utility functions are developed for all outputs of the RSEA module. As is common with consequence functions, the additive model is used to formulate the total utility function. Assuming utility independence, the overall unilateral utility function can be formed as (Ferreira, de Almeida, and Cavalcante 2009)

$$U_{t,j} = \sum_{i=1}^{n} w_i u_{ij(x)}; i = 1, \ldots, n; j = 1, \ldots, m \tag{9}$$

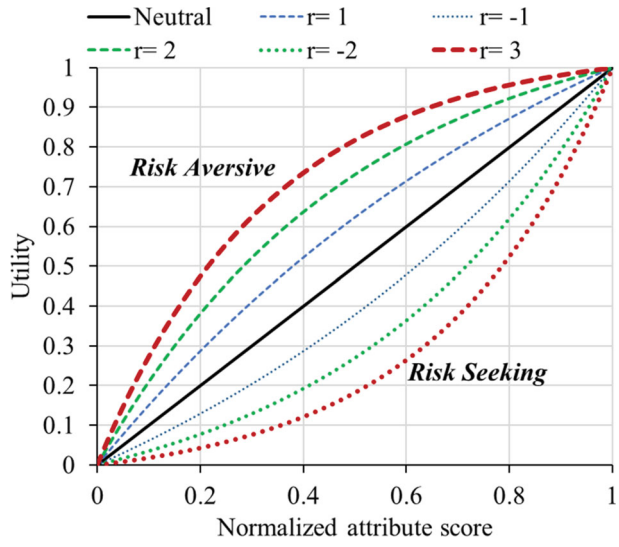

Figure 4. Utility curves with different attitude towards risk using exponential utility function adapted from (Wood and Khosravanian 2015).

where $U_{t,j}$ is the total utility of alternative j and w_i is the importance/weight factor (w_i). Decision maker uses lotteries between pairs of criteria to find w_i. w_i values are assigned based on historical data, engineering judgment and problem objective. Commonly, a numerical value between 1 (for equally important) and 9 (for absolutely more important) or their reciprocal is assigned to each pair of criteria to express the importance of one over the other. Similarly, 3, 5 and 7 mean objective i is weakly more important, strongly more important and very strongly more important than objective j, respectively (Mateo and Cristóbal 2012; Wallenius et al. 2008; Ferreira, de Almeida, and Cavalcante 2009). For instance, if the objective of the project is to minimize the asset loss, the decision maker compares the importance of the asset loss over the environmental loss and may assign a value of 9 to their pair to express absolute importance of the former over the later.

Objectives, scenarios and weight factors

A major advantage of multi-criteria decision models is their flexibility to deal with various decision scenarios, objectives and criteria. Here, seven scenarios with different objectives are studied: (1) minimum asset loss (AL), (2) minimum time loss (TL), (3) minimum life loss (LL), (4) minimum environmental loss (EL), (5) maximum resilience, (6) minimum annual operational energy cost (OEC) and (7) neutral scenarios. An example for Scenario 1, minimum AL, is a case where significantly valuable properties exist in the building, e.g. a warehouse with expensive stored asset. Scenario 2, minimum TL, applies to cases where the downtime is significantly costly and/or building should remain functional after an extreme event, e.g. building

is a hospital. Minimum LL, the objective of Scenario 3, is the primary goal of current design codes and is important particularly if a large number of people will reside or work in the building, for example if the building is a school. Scenario 4, minimum EL, is considered for a situation where due to client's requirements or official regulations the building should be eco-friendly. For Scenario 5, overall resilience of the building is the objective. Scenario 6 represents a case in a cold region with low seismicity where cost of energy is extremely high. For Scenario 7, all criteria have the same importance. The last scenario is assumed for comparison only.

Given the number of criteria involved and the interdependency between them, pairwise lotteries are used to find the w_i for each criterion over the others for various scenarios. Following previous studies on multi-criteria decision analysis (Ellingwood and Tekie 1999; Zavadskas et al. 2007), a survey was conducted among experts to find the w_i values. Participants include civil engineers, graduate students, and faculty members who were selected due to their familiarity with the topic. Participants were asked to select a weight factor to best represent the main goal of each scenario. The mean weight factor obtained from the survey is used, ignoring the upper and lower bounds of the data. Tables 1–6 list the pairwise comparison matrices and the weight factors for Scenarios 1–6, respectively. The w_i values for Scenario 7 are all 1/7.

Case studies

Design and numerical modelling of archetype RC buildings

Two groups of typical RC shear wall archetype buildings located in downtown Los Angeles, CA and Boston, MA are considered. In each group, three different configurations are considered to represent the typical shear

Table 1. Pairwise comparison matrix for Scenario 1 – minimum asset loss.

Criteria	AL	TL	LL	EL	ICC	OEC	MC	w_i for S1
AL	1	5	3	5	5	5	5	0.365
TL	1/5	1	1/3	2	2	3	2	0.103
LL	1/3	3	1	7	7	7	7	0.300
EL	1/5	1/2	1/7	1	2	3	2	0.082
ICC	1/5	1/2	1/7	1/2	1	1/2	1	0.045
OEC	1/5	1/3	1/7	1/3	2	1	2	0.059
MC	1/5	1/2	1/7	1/2	1	1/2	1	0.045

Table 2. Pairwise comparison matrix for Scenario 2 – minimum time loss.

Criteria	AL	TL	LL	EL	ICC	OEC	MC	w_i for S2
AL	1	1/2	1/2	3	3	3	3	0.155
TL	2	1	3	4	4	5	4	0.312
LL	2	1/3	1	6	7	7	7	0.298
EL	1/3	1/4	1/6	1	2	2	2	0.078
ICC	1/3	1/4	1/7	1/2	1	1/2	1	0.047
OEC	1/3	1/5	1/7	1/2	2	1	2	0.062
MC	1/3	1/4	1/7	1/2	1	1/2	1	0.047

Table 3. Pairwise comparison matrix for Scenario 3 – minimum life loss.

Criteria	AL	TL	LL	EL	ICC	OEC	MC	w_i for S3
AL	1	3	1/4	3	3	3	3	0.171
TL	1/3	1	1/7	1	2	2	2	0.084
LL	4	7	1	8	8	8	8	0.499
EL	1/3	1	1/8	1	2	3	2	0.091
ICC	1/3	1/2	1/8	1/2	1	1/2	1	0.046
OEC	1/3	1/2	1/8	1/3	2	1	2	0.063
MC	1/3	1/2	1/8	1/2	1	1/2	1	0.046

Table 4. Pairwise comparison matrix for Scenario 4 – minimum environmental loss.

Criteria	AL	TL	LL	EL	ICC	OEC	MC	w_i for S4
AL	1	3	1	1/4	3	2	3	0.158
TL	1/3	1	1/2	1/3	2	2	2	0.096
LL	1	2	1	1/3	6	6	6	0.225
EL	4	3	3	1	5	5	5	0.359
ICC	1/3	1/2	1/6	1/5	1	1/2	1	0.047
OEC	1/2	1/2	1/6	1/5	2	1	2	0.069
MC	1/3	1/2	1/6	1/5	1	1/2	1	0.047

Table 5. Pairwise comparison matrix for Scenario 5 – maximum resilience.

Criteria	AL	TL	LL	EL	ICC	OEC	MC	w_i for S5
AL	1	3	1	4	4	4	4	0.273
TL	1/3	1	1	2	3	3	3	0.160
LL	1	1	1	7	7	7	7	0.323
EL	1/4	1/2	1/7	1	2	3	2	0.088
ICC	1/4	1/3	1/7	1/2	1	1/2	1	0.046
OEC	1/4	1/3	1/7	1/3	2	1	2	0.063
MC	1/4	1/3	1/7	1/2	1	1/2	1	0.046

Table 6. Pairwise comparison matrix for Scenario 6 – minimum operational energy cost.

Criteria	AL	TL	LL	EL	ICC	OEC	MC	w_i for S6
AL	1	2	1/5	2	1/2	1/7	1/2	0.064
TL	1/2	1	1/5	1/2	1/2	1/7	1/2	0.040
LL	5	5	1	3	7	1	7	0.317
EL	1/2	2	1/3	1	1	1/8	1	0.065
ICC	2	2	1/7	1	1	1/6	1	0.070
OEC	7	7	1	8	6	1	6	0.373
MC	2	2	1/7	1	1	1/6	1	0.070

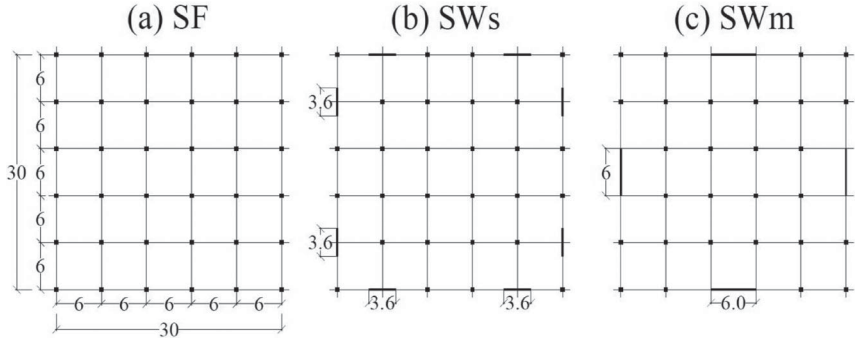

Figure 5. Floor plans of archetype RC building with different shear wall ratio: (a) SF archetype with no shear wall, (b) SWs archetype with 2 shear walls and (c) SWm archetype with one shear wall on each side (dimensions are in metres).

wall ratio of RC buildings. The LA site is selected for its extreme seismic activity but warm weather with S_s, spectral response acceleration at 0.2 s, and S_1, spectral response acceleration at 1 s, of 2.481 and 0.862 g, respectively, and ground snow load of 0–5 psf (0.24 kN/m^2). The Boston site is selected for its low seismicity but cold weather requiring considerable energy consumption, where S_s and S_1 are 0.217 and 0.069 g, respectively, and snow load of 40 psf (1.92 kN/m^2). All the archetype buildings for both Los Angeles and Boston share the same typical floor plans adapted from AlHamaydeh, Aly, and Galal (2017), see Figure 5. The building footprint is 30 m $\times$ 30 m, with 6 m long spans. The typical story height is 4 m. Two types of window glazing configurations, i.e. a double-pane glazing (BG) and a triple-pane low-e glazing (HG), are considered. The double-pane glazing represents the base line and the triple-pane low-e glazing represents a high-performance energy saving glazing. Archetypes are labelled based on location, configuration and glazing type. For example, LA-SF-BG is the archetype located in LA with a Special RC Moment Frame and base glazing. Similarly, B-SWm-HG is the archetype located in Boston with a shear wall in the middle of outer frames (see Figure 5c) and high-performance glazing.

Structures are designed based on ACI 318–14 (2014) and ASCE7-16 (2017). The designed RC frames are modelled in OpenSees (Mazzoni et al. 2006) as planar frames using fibre elements for beams and columns and SFI-MVLEM elements for shear walls. The SFI-MVLEM element recently developed by Kolozvari, Orakcal, and Wallace (2014) captures nonlinear interaction between shear and axial/flexural behaviour of RC walls and columns under cyclic loading. Models are validated with Tran and Wallace (2015) experiment on RC shear walls (Asadi 2020).

Specifications for life cycle cost analysis

The construction cost is calculated using Building Construction category of RSMeans (2018) considering both material and labour costs of different regions. The non-structural construction costs include the cost of exterior items such as windows and curtain walls as well as interior items such as partitions and ceiling. Installation costs

Table 7. Estimated life-cycle cost of studied archetypes.

Archetype	Initial construction cost (1000$)	Total replacement cost (1000$)	Cumulative maintenance cost in 50 years (1000$)
LA-SF-BG	7962	9954	3249
LA-SF-HG	8190	10,238	3363
LA-SWm-BG	8248	10,310	3249
LA-SWm-HG	8475	10,594	3363
LA-SWs-BG	8388	10,485	3249
LA-SWs-HG	8615	10,769	3363
B-SF-BG	7796	9746	3254
B-SF-HG	8026	10,033	3369
B-SWm-BG	8053	10,066	3254
B-SWm-HG	8283	10,353	3369
B-SWs-BG	8121	10,151	3254
B-SWs-HG	8351	10,439	3369

of windows are also estimated per RSMeans (2018), and glazing material costs differences are considered using Building Energy Optimization Tool (BEOpt) (Christensen et al. 2006). For maintenance costs, a commercial building template of Whitestone cost reference (Abate et al. 2009) is adapted given the occupancy of the buildings. It considers annual repair costs and periodic replacement costs of various structural and non-structural components. For instance, the replacement period of the glazing material is presumed 30 years and windowed curtain walls are assumed to have an annual cleaning/washing fee of 0.1 $/ft^2 in LA, and 0.11 $/ft^2 in Boston to account for slightly higher labour cost in Boston.

The seismic monetary loss is estimated as a Cumulative Distribution Function (CDF) of repair cost due to earthquake. The replacement cost is based on the construction cost estimated by RSMeans database (2018). This value includes the structure, exterior closure and utility infrastructure including HVAC cost and is called the core and shell replacement cost. The initial cost of HVAC is assumed the same for all cases and is not included in energy cost analysis. To account for tenant improvements and asset, this value is increased by 25% following FEMA P-58 assumptions for its example buildings (FEMA 2012). For estimating the downtime, a Total Replacement Time (TRT) of 720 days is considered. The maximum number of workers for repair is assumed 0.002 per ft^2 equal to 1 worker per 500 ft^2 (1 worker per 46.45 m^2) per FEMA recommendations (FEMA 2012). The initial construction, total replacement and 50-year cumulative maintenance costs are presented in Table 7. Note that the demolition costs are assumed to be the same for all the archetypes in either region and they are not studied as a criterion in the current study.

The main non-structural components considered in seismic loss estimation include two hydraulic elevators, one 350-Ton (BTU/h/12,000) chiller and air-handling unit on the roof, and a seismically rated independent pendant lighting for each 4-sq. m of the floor, perimeter stick-built curtain wall, interior gypsum wall partitions with metal studs, seismically rated raised access floor and suspended ceiling, and fire sprinkler. FEMA P-58 typically uses practical EDPs such as maximum interstory drift ratio (IDR) and maximum absolute floor acceleration (ACC) to catalogue damage state of structural and non-structural components. FEMA P-58 database is used to define the fragility specification for each component.

Energy analysis settings

Each floor of the archetype buildings is divided into nine thermal zones to study the influence of the shear wall distributions and building orientation on energy consumption and thermal comfort. The three-dimensional (3D) view of the special frame (SF) building and its thermal zones include a core of 18 m $\times$ 18 m at the centre and eight boundary zones on the perimeter of the building, as shown in Figure 6. The envelope, floor, HVAC, fenestration, etc. are designed per ASHRAE 90.1 requirements for the climate zones 3B (LA) with a Mediterranean climate and 5A (Boston) characterized by its cold and humid climate (ASHRAE 2016b; ASHRAE 2016a). The occupancy, lighting, equipment, ventilation and HVAC settings and schedules are adapted from ASHRAE reference building for middle and large office (ASHRAE 2016a). Following previous studies, the whole building architecture is modelled in DesignBuilder (DesignBuilder 2016) to create the input files for EnergyPlus (Crawley et al. 2001). The building has an occupancy of 18.51 m^2/person and lighting and office equipment intensities of 10.76 and 8.08 W/m^2, respectively. The HVAC system is a variable air volume (VAV) with reheat system. The AC heating and cooling setpoint temperature are 21.1°C (70°F) and 23.9°C (75°F) with heating back temperature of 15.6°C (60°F) and 29.4°C (85°F), respectively. The weather data of the Los Angeles International Airport (WMO #722950) and Boston-Logan International Airport (WMO #725090) are used as the input, which provides the seasonal temperature variations and precipitation schedules needed for building energy analysis.

The envelope, especially glazing materials play a critical role in the energy efficiency of window curtain wall buildings (Carmody and Haglund 2012). Solar heat gain coefficient (SHGC) and U-factor are the two most important parameters that differentiate window assemblies. While SHGC controls the transmission of solar heat through a window assembly, the *U*-value dictates the heat loss/gain of it. Lower *U*-factor can efficiently reduce the heat flow between indoor and outdoor space, and therefore saving energy consumption. The solar thermal properties and costs are listed in Table 8. The double-glazing represents a base case (BG) and costs of 267

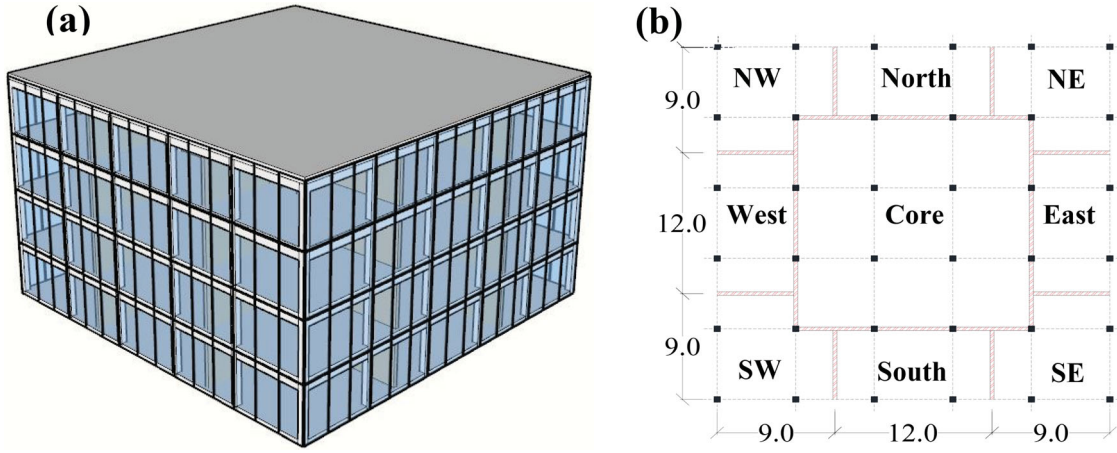

Figure 6. (a) SF archetype 3-dimentional (3D) view built in DesignBuilder and (b) typical thermal zone designation for all archetypes (dimensions in metres).

Table 8. Window glazing properties and costs.

Glazing	SHGC[a]	Direct solar transmission	Light transmission	U-value (W/m^2-K)	Cost ($/m^2$)
Double-pane glazing	0.25	0.21	0.31	2.58	267
triple-pane low-e glazing	0.14	0.07	0.30	1.07	394

[a]SHGC = Solar heat gain coefficient.

$/m^2, while the triple low-E glazing represents a high-performance case (HG) and costs of 394 $/m^2 (Christensen et al. 2006). For the SWs and SWm archetypes (see Figure 5b and c), the shear walls were insulated by a layer of EPS panel which was covered by a layer of stucco with the overall effective *U*-values of 0.53 and 0.40 W/m^2-K for archetypes located in Los Angeles and Boston respectively. To estimate CO_2 equivalent due to energy generation and the site energy (i.e. energy consumed by building) is converted into source energy using EnergyPlus conversion factors, which are 3.167 and 1.084 for electricity and natural gas, respectively. Kneifel (2010) indicated that the adoption of energy efficiency technologies (e.g. high-performance glazing) may lead to negative life cycle cost because the improved energy efficiency allows the installation of smaller and cheaper HVAC equipment. In this study, it is assumed that different building archetypes adopt the same HVAC system and share the same initial installation costs.

Seismic fragility analysis

For dynamic analysis in OpenSees, a set of 22 far-field (located at greater than or equal to 10 km from the fault rupture site) ground motions recommended by FEMA P-695 (ATC 2009) for collapse analysis are used. Records are on soft rock and stiff soil (Site Class C and D) with magnitudes between M6.5 and M7.6 taken from 14 different events (Asadi and Adeli 2018). The records are normalized with respect to PGV and scaled such that the median spectrum of the record set matches the design response spectrum (ASCE 2017; ATC 2009).

Incremental Dynamic Analysis (IDA), a widely accepted method to study the record-to-record variability of earthquake hazard, is used to evaluate performance and collapse capacity of the archetypes (Azarbakht and Dolšek 2010). The collapse capacity, $\hat{S}_{CT}$, obtained from IDA is used to find the empirical CDF of collapse fragility functions. Then, maximum likelihood method is used to fit a lognormal distribution function over the empirical CDF. The empirical CDF and the fitted lognormal collapse curve are illustrated in Figure 7 for various archetypes where horizontal axis shows the normalized pseudo-spectral acceleration based on 5% damped design spectra for the region at the fundamental period of the building structure, i.e. $S_a(T_1, 5\%)$. Table 9 summarizes the expected collapse capacity and IDR and their logarithmic dispersion (β). All archetypes marginally satisfy ASCE7-16 (ASCE 2017) requirement for the conditional probability of failure caused by the maximum considered earthquakes (MCE), which is 10% for risk category of I. Note that the glazing type of curtain walls is assumed to have little impact on the collapse capacity. As expected, the LA archetypes achieve a considerably larger collapse capacity, $S_a(T_1,5\%)$, compared to Boston archetypes given LA archetypes are designed for a high seismic region. In contrast, IDR at collapse is close for LA and Boston

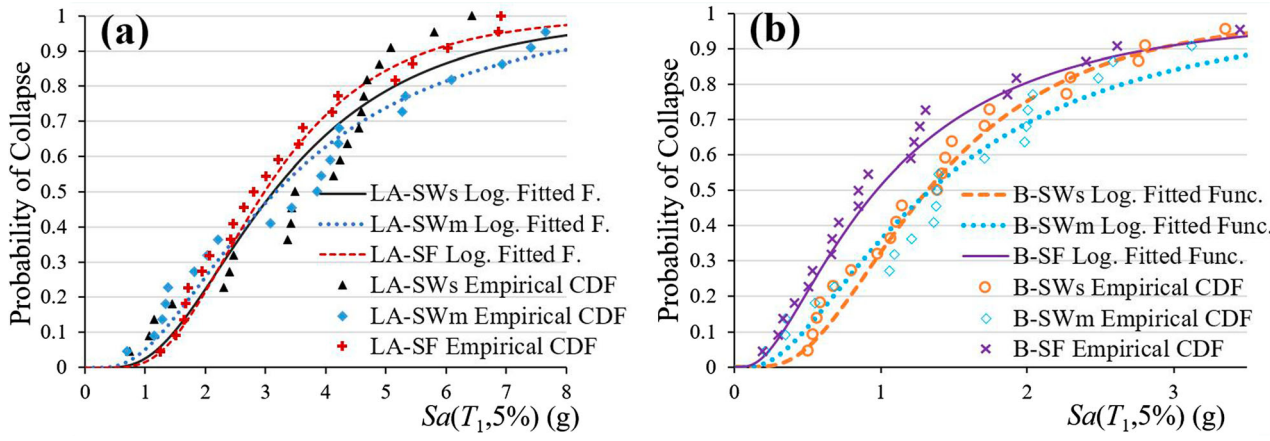

Figure 7. Empirical CDF of $S_a(T_1,5\%)$ and fitted lognormal fragility functions for (a) LA and (b) Boston archetypes.

Table 9. Expected collapse capacity and collapse IDR and their corresponding logarithmic dispersion.

Archetype	$S_{CT}(T_1,5\%)$ (g)	$\beta_{S_{CT}}$	Collapse IDR (%)	β_{IDR}
LA-SF	2.98	0.51	7.13	0.46
LA-SWm	3.17	0.71	0.82	0.87
LA-SWs	3.13	0.59	0.79	0.63
B-SF	0.97	0.84	6.55	0.66
B-SWm	1.34	0.81	0.71	1.08
B-SWs	1.32	0.61	0.85	0.46

archetype because IDR at collapse is an indicator of structural system, which is a special moment frame or special moment frame combined with shear walls, and not the region.

Seismic loss estimation

FEMA PACT database of fragility parameters, repair cost/time, casualty and fatality consequence function for various structural and non-structural components are used to perform Monte Carlo simulations for loss estimation (FEMA 2012). The resilience metrics including the component-level direct economic loss, downtime and number of casualty (injuries and fatality) caused by intensity-based and time-based earthquake hazard are evaluated. The direct economic loss is calculated as the summation of repair/replacement costs of all structural and non-structural components. Similarly, the downtime is the summation of repair time required for all components on each floor. Two repair planning schemes: slow-track (serial planning) and fast-track (parallel planning) are considered for downtime analysis. As noted, a commercial population model is considered for the building to estimate the casualty. Considering the unoccupied areas such as utility and mailing room, 1/3 of the first floor and 1/6 of other floors are assumed unoccupied (Han, Li, and van de Lindt 2016). The component-level casualty consequence functions of FEMA PACT are used for casualty estimation.

Time to repair the damages caused by earthquakes and restore the functionality of the building is a main indicator of the robustness and resilience of the system. Figures 8 and 9 depict the cumulative annual repair time and the number of injuries for various archetypes considering a fast-track repair scheme, respectively. As expected, earthquake causes an insignificant annual loss for Boston archetypes compared to LA ones. For instance, the annual probability of repair time exceeding 10 days for the B-SF-BG archetype is about 0.00047, much smaller than that of the corresponding LA case (LA-SF-BG) which is 0.078. As shown in Figures 8 and 9, glazing type has little impact on repair time and casualty. However, it has a minor impact on the repair cost.

Shear walls have a major impact on all losses. In both cities, framed RC buildings require a longer repair/replacement time compared to that of shear wall archetypes. This is true for repair/replacement costs as well, but not for injuries and fatalities due to earthquake. RC framed buildings, SF archetypes, have much smaller lateral stiffness compared to the shear wall RC buildings. This leads to a noticeable increase in IDR and considerable damage to non-structural components even in low seismic intensities (0.05–0.2 g) as shown in Figure 10. Figure 10 shows the annual rate of exceedance of repair cost and fatalities for LA-SF-BG archetype. The horizontal axes show the earthquake intensity in terms of $S_a(T_1,5\%)$ and the loss in terms of repair cost (Figure 10a) or number of fatalities (Figure 10b). As depicted, most of the monetary loss and downtime of RC buildings at a high seismic region like LA is due to low- to mid-intensity earthquakes with $S_a(T_1,5\%)$ between 0.1 and 0.6 g. Note that while the ground motion intensity is not significant in that range, the mean annual frequency of exceedance (MAFE) of that intensity range is significant, i.e. about 0.02 or a return period of 50 years. At

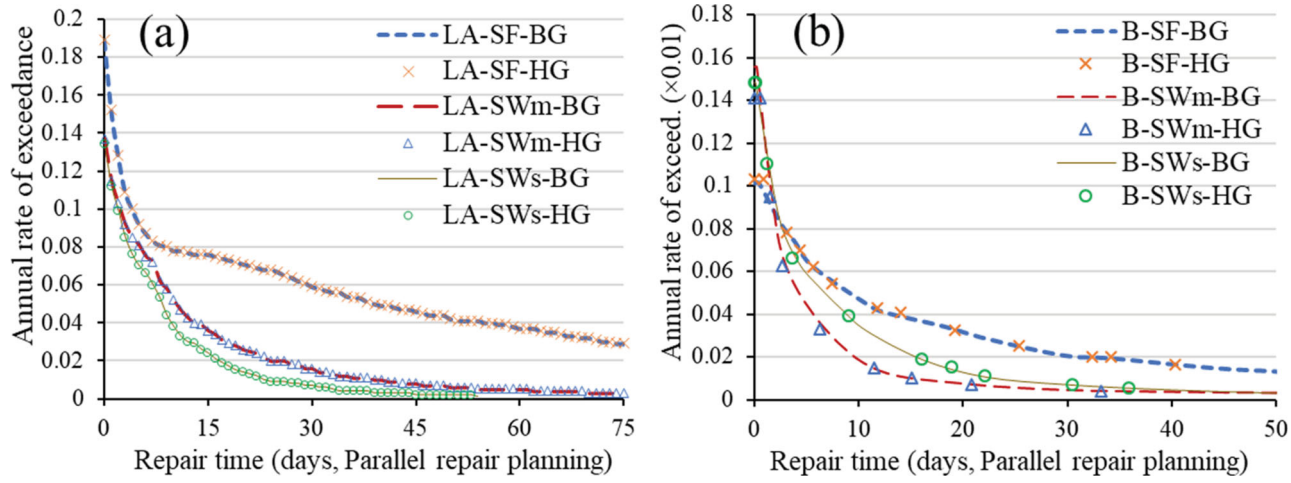

Figure 8. Cumulative annual repair time for various (a) LA and (b) Boston archetypes.

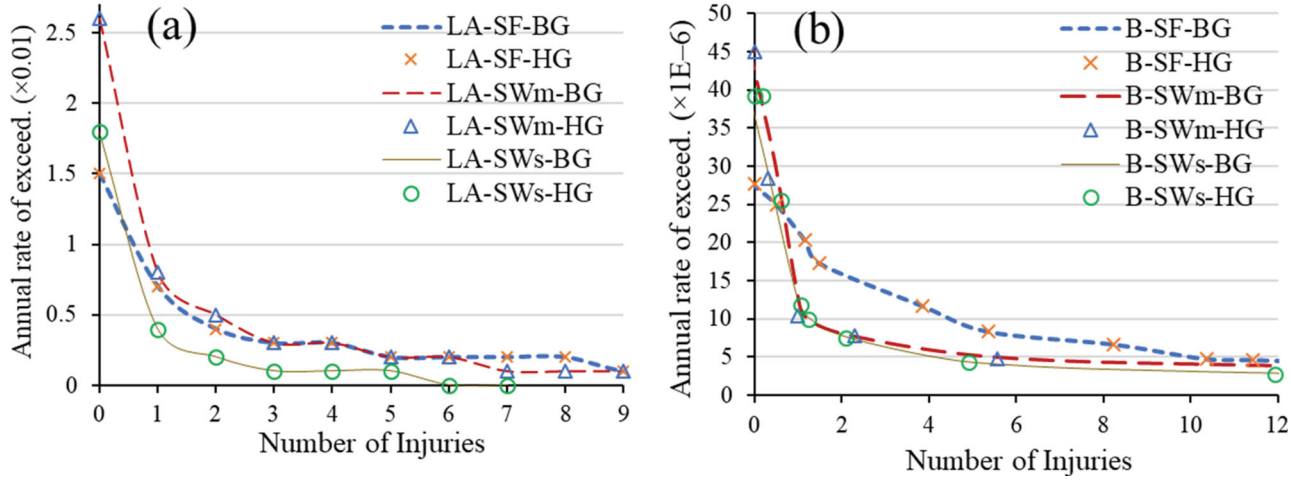

Figure 9. Cumulative annual number of injuries for various (a) LA and (b) Boston archetypes.

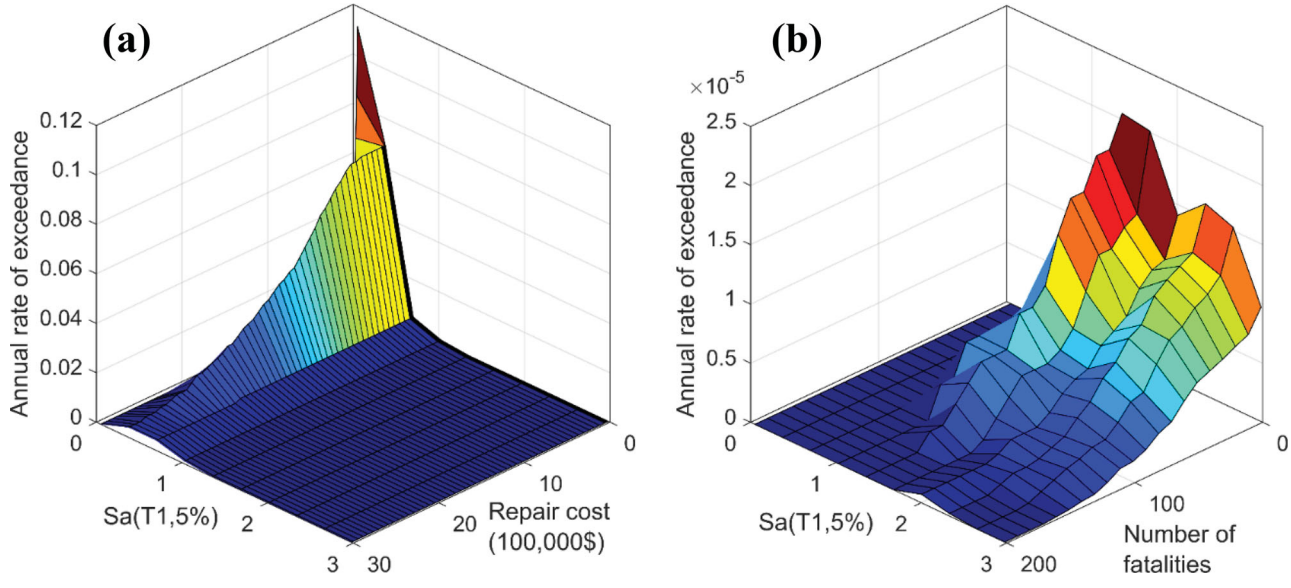

Figure 10. Annual rate of exceedance of (a) repair cost and (b) fatalities for LA-SF-BG archetype.

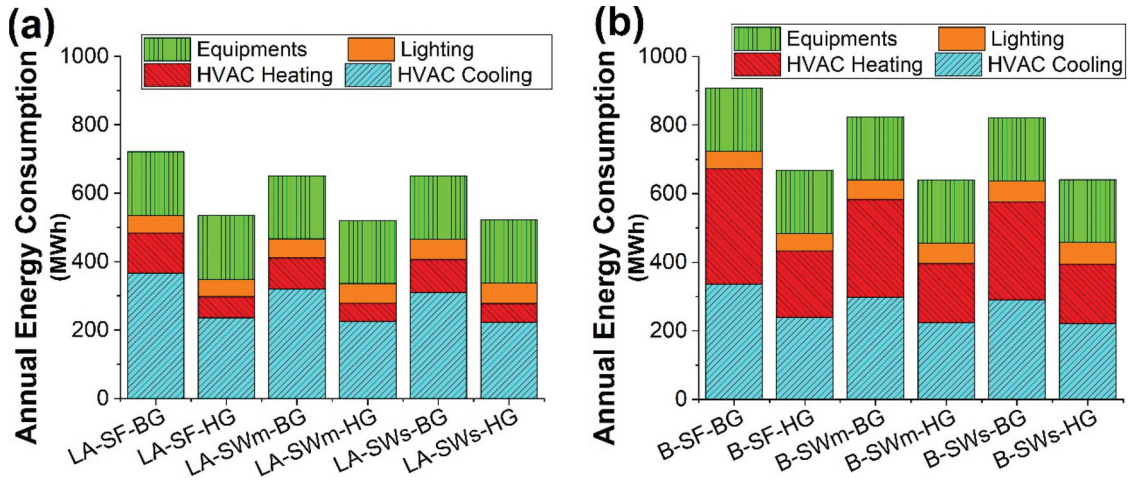

Figure 11. Annual energy consumptions for various archetype buildings in regions: (a) Los Angeles and (b) Boston.

low to mid intensities, non-structural components such as wall partitions and suspended ceilings are the main contributor to the loss and casualty.

Energy cost analysis and CO_2 eq emissions

The whole-building energy analysis is performed in EnergyPlus (Crawley et al. 2001) and the annual energy consumptions are obtained. Figure 11 compares the energy consumption for HVAC cooling and heating, lighting and equipment for various archetypes of LA and Boston. For comparison, the annual energy consumption of the building with a similar setting (window wall ratio of 37.5%, base window glazing and lightweight wall with effective *U*-value 0.41 W/m^2-K) is 134 kWh/m^2 which lies in the range of PNNL benchmark case of a medium to a large office with annual energy consumption of 77–196 kWh/m^2 for climate zone 3. As depicted, heating constitutes the major part of annual energy use in Boston while cooling is a significant end use for both sites. The RC framed buildings consume noticeably more energy for both cooling and heating compared to shear wall cases (16% and 14% less on average for LA and Boston buildings with BG, respectively). The difference is less significant for HG, high performance glazing, though (6% and 9% less HVAC energy use on average for LA and Boston buildings with HG, respectively). This is mainly caused by the combined effects of the thermal mass and shading effects of shear walls. It highlights the positive influence of shear walls on energy consumption in addition to their advantages in terms of structural performance and overall monetary loss and downtime, as discussed earlier. Yet, the energy use for lighting increases in shear wall buildings since solid shear walls reduce the natural light entering the building. Given that lighting is a minor part of annual energy use compared to HVAC, shear walls archetypes have a clear advantage in terms of energy consumption. In general, SWs archetypes show smaller energy use for HVAC than SWm archetypes. However, this difference is also slightly diminished by the increase in energy use for lighting. Table 10 summarizes the energy consumption and cost and CO_2 eq emission due to energy consumption for various archetypes.

Table 10. Annual energy consumption, cost and CO_2 eq emission due to energy consumption for various archetypes.

Archetype	Consumption (MWh)	Cost (1000$)		CO_2 eq (ton)
		Electricity	Natural Gas	
LA-SF-BG	721	109	5	177
LA-SF-HG	533	85	3	133
LA-SWm-BG	651	101	4	162
LA-SWm-HG	522	85	2	130
LA-SWs-BG	650	100	4	161
LA-SWs-HG	524	85	2	131
B-SF-BG	907	125	15	316
B-SF-HG	670	104	9	247
B-SWm-BG	826	118	13	293
B-SWm-HG	641	103	8	240
B-SWs-BG	823	117	13	291
B-SWs-HG	643	103	8	240

Figure 12 depicts the annual energy costs due to various uses for various archetypes. Due to difference in type of energy (i.e. electricity or gas) used, the energy cost of heating is noticeably smaller than energy cost of cooling. Similar to energy consumption, the buildings with shear wall show smaller overall energy cost compared to framed buildings for both sites. The difference is more significant for Boston, particularly for heating cost. Considering the source and type of energy in LA and Boston, the annual CO_2 eq emission due to energy used is also presented in Table 10. Note that the labour costs are different for considered location, structural frame, and to a lesser extent glazing alternative. The labour cost impact is evident in Figure 12 and Table 10. Note that, location-based

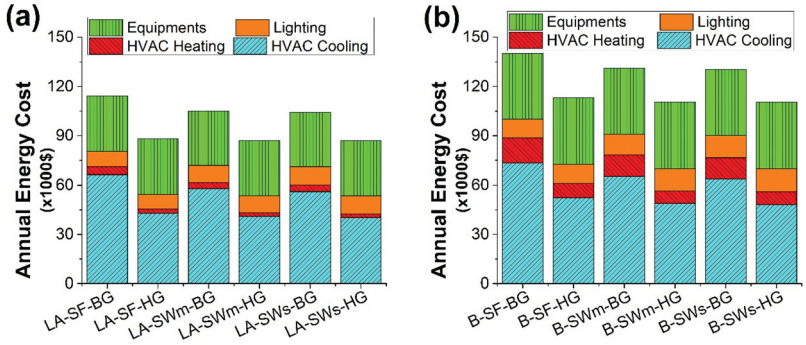

Figure 12. Annual energy costs for various archetype buildings in regions: (a) Los Angeles and (b) Boston.

cost indices are used for energy analysis to reflect the impact of labour costs in different locations (Los Angeles compared with Boston). Moreover, the cost database of RSMeans, FEMA P-58 and Whitestone, which are used here, all consider the labour cost in their estimated cost for various building components.

The properties of the glazing determine the solar heat gain, direct solar transmission and light transmission of heat and light from windows. Note that glazing significantly affects the heating and cooling energy use, energy cost and CO_2 eq emission. Using high-performance triple-pane low-e glazing (i.e. HG cases) reduces the energy use, cost and CO_2 eq emission between 27% and 38% compared to double-pane glazing (i.e. BG cases) for HVAC heating and cooling. As such, while glazing has little impact on resilience, it has a significant impact on sustainability and energy consumption. These conflicting criteria of BG and HG archetypes can be better studied in a multi-criteria decision-making framework.

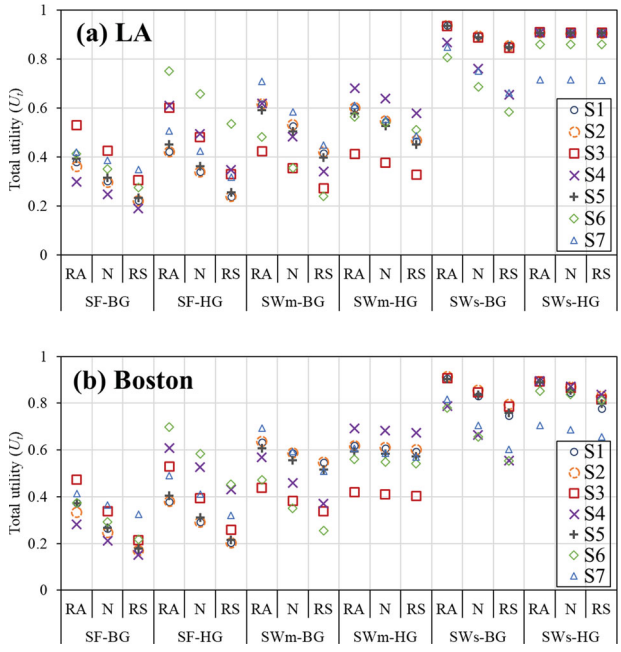

Figure 13. Total utility (U_t) scores for various scenarios for (a) LA and (b) Boston buildings with risk aversive (RA), neutral (N), and risk seeking (RS) attitudes.

Risk-informed multi-criteria decision making

The proposed decision model is used to find the optimal choice among all design alternatives. All criteria quantified in the RSEA module are the input parameters of the decision-making module, listed in Tables 11 and 12 for LA and Boston archetypes, respectively. For life loss (LL), the weighted addition method is used to combine the annual injury and fatality outputs (Mateo and Cristóbal 2012). To reflect the significance of fatality over injuries in total LL, a weight factor of 15 is assumed for fatalities. This factor is based on the difference between fatality comprehensive cost and mean injury comprehensive cost suggested by FHWA (1994) and Sutley, van de Lindt, and Peek (2016). Environmental loss (EL) is the GHG emissions due to initial construction, seismic repair/replacement, maintenance activities and operational energy consumption.

Risk is also incorporated in the decision model through decision maker's attitudes towards risk, which can be risk aversion, neutral or risk seeking. Based on the objective/s of the project, the decision-maker may take or avoid a certain level of risk in decision analysis. This improves the adaptability of the model in dealing with subjective and conflicting criteria and provides new avenues to stakeholders in risk and resource management. The level of risk can be adjusted with factor r in Equation (8). Figure 13 and Tables 11 and 12 show the total utility (U_t) scores for various cases studied. For demonstration, an r factor of 2 is used in these tables and figure.

For most scenarios, the RC buildings with two shear walls (SWs-BG and SWs-HG archetypes) are the best alternatives as they achieved the highest scores. This is mostly due to their small seismic loss (monetary cost, downtime and casualty) as well as their comparable energy costs compared to other archetypes. The high score of those archetypes is more evident for Scenarios 1–3 where

Table 11. Evaluation matrix obtained from RSEA module and total utility (U_t) scores for various scenarios with risk aversive (RA), neutral (N), and risk seeking (RS) attitudes for LA archetypes.

	LA-SF-BG			LA-SF-HG			LA-SWm-BG			LA-SWm-HG			LA-SWs-BG			LA-SWs-HG		
Criteria	Annual seismic resilience criteria																	
AL (10^3\$)	148.4			153.8			50.6			50.8			31.8			32.0		
TL (days)	7.126			7.130			2.276			2.276			1.477			1.477		
LL (# of Casualties)	0.050			0.050			0.078			0.078			0.036			0.036		
	Life-cycle Sustainability Criteria																	
EL (ton CO_2e)																		
EL – Const.	4,690			4,820			4,860			4,990			4,940			5,070		
EL – M & R[a]	6,660			6,900			3,610			3,680			3,020			3,100		
EL – OE[b]	41,761			32,494			38,539			32,156			38,261			32,169		
ICC (10^3\$)	7,963			8,190			8,248			8,475			8,388			8,615		
MC (10^3\$)	3,249			3,363			3,249			3,363			3,249			3,363		
	Life-cycle Energy Criterion																	
OEC (10^3\$)	4,627			3,555			4,251			3,513			4,221			3,513		
Scenarios	Total utility (U_t) scores with risk aversive (RA), neutral (N), and risk seeking (RS) attitudes																	
	RA	N	RS	RA	N	RS	RA	N	RS	RA	N	RS	RA	N	RS	RA	N	RS
S1	0.380	0.303	0.223	0.421	0.340	0.239	0.615	0.527	0.416	0.600	0.544	0.464	0.938	0.895	0.856	0.909	0.909	0.909
S2	0.361	0.296	0.222	0.421	0.340	0.240	0.617	0.531	0.422	0.601	0.547	0.468	0.937	0.894	0.854	0.906	0.906	0.906
S3	0.529	0.425	0.305	0.601	0.480	0.331	0.424	0.353	0.272	0.413	0.377	0.329	0.934	0.888	0.845	0.908	0.908	0.908
S4	0.299	0.248	0.191	0.609	0.494	0.347	0.618	0.484	0.340	0.682	0.639	0.578	0.868	0.761	0.654	0.906	0.906	0.906
S5	0.392	0.316	0.233	0.450	0.363	0.255	0.591	0.505	0.397	0.578	0.526	0.450	0.934	0.889	0.847	0.907	0.907	0.906
S6	0.414	0.351	0.275	0.751	0.657	0.535	0.482	0.356	0.239	0.564	0.539	0.511	0.805	0.687	0.585	0.859	0.859	0.859
S7	0.420	0.386	0.348	0.506	0.423	0.319	0.707	0.583	0.448	0.612	0.554	0.486	0.849	0.750	0.661	0.714	0.714	0.714

[a]Environmental consequences due to maintenance activities and seismic damage repair.
[b]Environmental consequences due to operational energy use.

Table 12. Evaluation matrix obtained from RSEA module and total utility (U_t) scores for various scenarios with risk aversive (RA), neutral (N), and risk seeking (RS) attitudes for Boston archetypes.

	B-SF-BG			B-SF-HG			B-SWm-BG			B-SWm-HG			B-SWs-BG			B-SWs-HG		
Criteria	Annual seismic resilience criteria																	
AL (10^3\$)	0.4864			0.5046			0.3173			0.3217			0.3409			0.3440		
TL (Days)	0.0255			0.0255			0.0163			0.0163			0.0164			0.0164		
LL (# of Casualties)	4.47E-4			4.48E-4			4.96E-4			4.98E-4			3.87E-4			3.91E-4		
	Life-cycle sustainability criteria																	
EL (ton CO_2e)																		
EL – Const.	4590			4730			4740			4880			4780			4920		
EL – M & R[a]	2050			2120			2040			2110			2040			2110		
EL – OE[b]	48,740			40,299			45,970			39,593			45,670			39,601		
ICC (10^3\$)	7796			8026			8053			8283			8121			8351		
MC (10^3\$)	3254			3369			3254			3369			3254			3369		
	Life-cycle energy criterion																	
OEC (10^3\$)	5734			4612			5359			4500			5326			4500		
	Total utility (U_t) scores with risk aversive (RA), neutral (N), and risk seeking (RS) attitudes																	
Scenarios	RA	N	RS	RA	N	RS	RA	N	RS	RA	N	RS	RA	N	RS	RA	N	RS
S1	0.374	0.264	0.173	0.379	0.292	0.202	0.634	0.585	0.547	0.618	0.606	0.592	0.905	0.832	0.747	0.887	0.845	0.777
S2	0.333	0.246	0.169	0.379	0.291	0.202	0.636	0.587	0.549	0.619	0.610	0.602	0.914	0.855	0.795	0.893	0.869	0.829
S3	0.473	0.337	0.215	0.529	0.393	0.259	0.437	0.381	0.338	0.420	0.411	0.403	0.908	0.847	0.786	0.893	0.865	0.816
S4	0.282	0.212	0.152	0.609	0.527	0.432	0.568	0.458	0.371	0.692	0.683	0.675	0.787	0.665	0.555	0.894	0.873	0.836
S5	0.373	0.267	0.178	0.405	0.312	0.216	0.607	0.556	0.515	0.594	0.584	0.572	0.904	0.835	0.760	0.889	0.854	0.798
S6	0.374	0.292	0.217	0.698	0.583	0.454	0.472	0.351	0.255	0.560	0.550	0.542	0.780	0.657	0.553	0.852	0.838	0.813
S7	0.414	0.365	0.324	0.490	0.411	0.321	0.693	0.594	0.510	0.606	0.586	0.570	0.817	0.705	0.602	0.705	0.686	0.656

[a]Environmental consequences due to maintenance activities and seismic damage repair.
[b]Environmental consequences due to operational energy use.

the objective is to minimize seismic asset, time and life losses. They have the least AL, TL and LL making them the best alternative for LA site. However, from a sustainability viewpoint, the initial construction cost of archetypes with shear wall is slightly larger than framed buildings (up to 5%). In an MCDM framework, all these conflicting outputs can be taken into account, systematically. As such, the minor difference in initial cost does not affect the overall utility score. Note that the significant thermal mass of shear walls helps with energy consumption as well reducing the cost of operational energy and improves the scores for SWs and SWm alternatives.

As shown in Figure 13, the U_t scores for scenarios 1, 2 and 5 (minimum asset loss and time loss and maximum resilience) for both sites follow a very similar variation. This indicates the close interdependency between the AL, TL and resilience in general. Scenario 3, minimum casualty, changes differently for various archetypes. For Scenario 3, the U_t scores of LA-SF are noticeably larger than that of LA-SWm. The difference is more evident in the risk aversion case. This is mainly due to smaller LL in the case of RC framed buildings compared to buildings with one centreline shear wall on each side. It is also partly due to the importance/weight factor assigned to life loss. In the survey conducted to quantify the weight factors, most participants gave a larger pairwise importance factor to life loss compared to other losses such as AL or TL. In general, the factors adjust the significance of a criterion compared to others based on decision-maker's or stakeholder's preferences.

For all cases, averting risk results in a higher score, as expected. But, this change to scores differs from one archetype to another. For SF archetypes, the U_t score drops noticeably if the decision-maker wants to seek risk whereas for SWm and SWs cases, the U_t score decreases slightly. The drop in U_t scores is generally less significant for archetypes with high-performance glazing (HG cases). HG archetypes achieve a better score than archetypes with base glazing (BG) for most scenarios considering the conflicting factors of initial cost and energy consumed. For Scenario 6, in particular, where minimum operational energy is the objective, they achieve a considerably larger score (between 7% larger in the case of LA-SWs with risk aversion attitude to 214% larger in the case of LA-SWm with risk-seeking attitude). The change in utility score from RA to N attitude is not the same as the change in utility score from N to RS attitude. Also, the rate of this change varies from one archetype to another and is noticeably less significant for the LA-SWs-HG archetype. Comparing the outputs for various alternatives, it was found that if the outputs for two criteria are conflicting (one output is ideal and another is non-ideal) this rate increases whereas having consistent outputs for all criteria (all ideal or non-ideal values) decreases this rate. This shows the ability of the framework to integrate various conflicting criteria into risk-based decision making.

Conclusion

This paper presents a novel multi-criteria framework for the design of buildings considering various resilience, sustainability and energy criteria. Building upon recent advances in loss analysis and energy simulation, it provides a new quantitative risk-based decision model for integrated structural and architectural performance assessment and design. Given the trade-off between various criteria involved in the design of a built environment, a multi-criteria decision model is proposed to quantitatively integrate their impacts. Though well-established, multi-criteria decision models (MCDM) have rarely been used in seismic resilience assessment particularly when sustainability and energy are included. To achieve a comprehensive framework, key factors from each aspect of building performance are integrated into the model. Factors such as seismic repair cost, repair time, injuries, fatalities, construction and maintenance costs, embodied energy, and operational energy are studied. Several uncertainties are also considered, including uncertainty in record-to-record variability, consequence function and modelling. In addition to uncertainties considered, we have proposed a risk aversion factor to the utility model which provides the ability to adjust risk in decision analysis.

Pairwise lotteries should be used to find the weight factors in decision analysis. A survey is conducted to quantify recommended weight factors for seven different scenarios/objectives. These factors may be adjusted to integrate stakeholders' preferences. Moreover, decision-makers can manage the level of risk they may accept or avoid in the analysis by adjusting the risk aversion factor (r). Architects and structural designers may use the proposed framework to study, compare, and contrast available alternatives in detail and rank them based on stakeholders' preference and level of risk they may accept or avoid. Furthermore, policymakers may use the framework to promote the use of specific structural or non-structural components in specific regions or buildings considering a comprehensive list of resilience, sustainability, and energy criteria.

Though the proposed framework can be used for essentially any building archetype, it is most suitable for comparing various design alternatives of low- to mid-rise multi-story residential or commercial buildings. Lack of publicly accessible data on tall buildings or special buildings such as hospitals and schools can limit the usability of the current framework for such cases. In this

study, the framework is implemented on RC buildings in two geographic locations with different seismic intensities and climate conditions and the impact of shear wall ratios on the asset, time, life and environmental losses as well as energy consumption is studied.

Compared to RC buildings with shear walls, RC framed buildings consumed noticeably more energy for cooling and heating (on average 12%). This is partly due to the shading effect provided by the wall and, to a lesser extent, due to the significant thermal mass of shear walls. Archetype buildings with shear wall experience less monetary seismic loss and downtime as well resulting in high total utility scores in the decision analysis. As such, for most cases, buildings with symmetric side shear walls ranked first in decision analysis even though they require a higher initial construction cost. Nonetheless, shear walls block the natural light resulting in slightly more energy use for lighting. Further, glazing has little impact on resilience but a significant influence on heating and cooling energy use and cost. As such, using triple-pane low-e glazing reduced the energy use, cost and corresponding CO_2 eq. emission as much as 48% compared to regular double-pane glazing. Averting risk results in a higher utility score, particularly in the case of regular double glazing. As discussed, these trade-off between various criteria, i.e. different cost, loss and energy criteria, can be studied in a multi-criteria framework even if they yield conflicting outputs.

As an extension to this study, multi-variable formal optimization techniques can be used to find the optimal member size, location and cost given various economic, social and environmental criteria such as estimated direct/indirect loss or cradle to grave cost. Nature-based algorithms for global optimization such as swarm intelligence, multi-agent models based on the behaviour of social swarm, evolutionary computation, and multi-dimensional models based on biological evolution theory can be used for such studies (Ekici et al. 2019; Jafari and Valentin 2018; Sutley, van de Lindt, and Peek 2016; Wang et al. 2019). Furthermore, the trilateral decision model proposed here can be applied to other structure or infrastructure systems as well and be the basis for a computer program which automatically makes decisions on structural and architectural design/retrofit projects.

Uncertainty in seismic analysis stems largely from variability in ground motion properties and uncertainty in performance specification of structural and non-structural components, which are included in this paper. However, as a limitation of this study, other factors contributing to risk such as uncertainty in material and geometric properties, uncertainty in modelling methodologies and assumptions, and upper and lower bounds of each factor are not explicitly studied. These factors may affect the utility scores and the optimal decision. Balancing a practical level of uncertainty and an acceptable computational effort can be a topic of future studies as well (Jamie Ellen Padgett and DesRoches 2007).

Disclosure statement

No potential conflict of interest was reported by the author(s).

ORCID

Esmaeel Asadi http://orcid.org/0000-0002-8796-5408

References

Abate, D., M. Towers, R. Dotz, and L. Romani. 2009. "The Whitestone Facility Maintenance and Repair Cost Reference 2009-2010." Whitestone Research, California.

ACI 318-14. 2014. *Building Code Requirements for Structural Concrete (ACI 318-14) and Commentary*. Edited by Reported by ACI Committee 318. Vol. 11. MI: American Concrete Institute.

AlHamaydeh, Mohammad, Nader Aly, and Khaled Galal. 2017. "Impact of Seismicity on Performance and Cost of RC Shear Wall Buildings in Dubai, United Arab Emirates." *Journal of Performance of Constructed Facilities* 31 (5): 04017083. doi:10.1061/(ASCE)CF.1943-5509.0001079.

Asadi, Esmaeel. 2020. "Risk-Informed Multi-Criteria Decision Framework for Resilience and Sustainability Assessment of Building Structures." Case Western Reserve University. https://etd.ohiolink.edu/pg_10?0::NO:10:P10_ACCESSION_NUM:case1575381834399844.

Asadi, Esmaeel, and Hojjat Adeli. 2018. "Nonlinear Behavior and Design of Mid-to-Highrise Diagrid Structures in Seismic Regions." *Engineering Journal, American Institute of Steel Construction* 55 (3): 161–180.

Asadi, Esmaeel, Yue Li, and H. YeongAe. 2018. "Seismic Performance Assessment and Loss Estimation of Steel Diagrid Structures." *ASCE Journal of Structural Engineering* 144: 10. doi:10.1061/(ASCE)ST.1943-541X.0002164.

Asadi, Esmaeel, Abdullahi M. Salman, and Yue Li. 2019. "Multi-Criteria Decision-Making for Seismic Resilience and Sustainability Assessment of Diagrid Buildings." *Engineering Structures* 191 (July): 229–246. doi:10.1016/j.engstruct.2019.04.049.

ASCE. 2017. *Minimum Design Loads and Associated Criteria for Buildings and Other Structures*. ASCE/SEI Standard No. 7-16, American Society of Civil Engineers, Reston, Virginia. doi:10.1061/9780784414248.

ASHRAE. 2016a. "Energy Standard for Buildings Except Low-Rise Residential Buildings." *ANSI/ASHRAE/IES Standard 90.1*-2016: 90.

ASHRAE. 2016b. "Weather Data for Building Design Standards." *ANSI/ASHRAE Standard* 169: 169.

ATC. 2009. "Quantification of Building Seismic Performance Factors." *Fema*, P695., no. June: 421.

Azarbakht, Alireza, and Matjaž Dolšek. 2010. "Progressive Incremental Dynamic Analysis for First-Mode Dominated Structures." *Journal of Structural Engineering* 137 (3): 445–455.

Baglivo, Cristina, Paolo Maria Congedo, and Andrea Fazio. 2014. "Multi-Criteria Optimization Analysis of External Walls According to ITACA Protocol for Zero Energy Buildings in

the Mediterranean Climate." *Building and Environment* 82 (December): 467–480. doi:10.1016/j.buildenv.2014.09.019.

Basbagill, J., F. Flager, M. Lepech, and M. Fischer. 2013. "Application of Life-Cycle Assessment to Early Stage Building Design for Reduced Embodied Environmental Impacts." *Building and Environment* 60 (February): 81–92. doi:10.1016/j.buildenv.2012.11.009.

Belleri, Andrea, and Alessandra Marini. 2016. "Does Seismic Risk Affect the Environmental Impact of Existing Buildings?" *Energy and Buildings* 110 (January): 149–158. doi:10.1016/j.enbuild.2015.10.048.

Bocchini, Paolo, M. Asce, Dan M Frangopol, Dist M Asce, Thomas Ummenhofer, and Tim Zinke. 2014. "Resilience and Sustainability of Civil Infrastructure : Toward a Unified Approach." *Journal of Infrastructure Systems*, doi:10.1061/(ASCE)IS.1943-555X.0000177.

Bruneau, Michel, Stephanie E. Chang, Ronald T. Eguchi, George C. Lee, Thomas D. O'Rourke, Andrei M. Reinhorn, Masanobu Shinozuka, Kathleen Tierney, William A. Wallace, and Detlof Von Winterfeldt. 2003. "A Framework to Quantitatively Assess and Enhance the Seismic Resilience of Communities." *Earthquake Spectra* 19 (4): 733–752.

Carmody, John, and Kerry Haglund. 2012. *Measure Guideline: Energy-Efficient Window Performance and Selection*. Golden, CO: National Renewable Energy Lab.(NREL).

Chau, C. K., T. M. Leung, and W. Y. Ng. 2015. "A Review on Life Cycle Assessment, Life Cycle Energy Assessment and Life Cycle Carbon Emissions Assessment on Buildings." *Applied Energy* 143 (April): 395–413. doi:10.1016/j.apenergy.2015.01.023.

Christensen, C., R. Anderson, S. Horowitz, A. Courtney, and J. Spencer. 2006. *BEopt(TM) Software for Building Energy Optimization: Features and Capabilities. NREL/TP-550-39929*. Golden, CO: National Renewable Energy Lab. (NREL). doi:10.2172/891598.

Cimellaro, Gian Paolo, Andrei M. Reinhorn, and Michel Bruneau. 2010. "Framework for Analytical Quantification of Disaster Resilience." *Engineering Structures* 32 (11): 3639–3649.

CMU GDI. 2018. *Economic Input-Output Life Cycle Assessment (EIO-LCA), US 2002 Economic Benchmark Model Last Update* 2010. http://www.eiolca.net.

Crawley, Drury B., Linda K. Lawrie, Frederick C. Winkelmann, Walter F. Buhl, Y. Joe Huang, Curtis O. Pedersen, Richard K. Strand, Richard J. Liesen, Daniel E. Fisher, and Michael J. Witte. 2001. "EnergyPlus: Creating a New-Generation Building Energy Simulation Program." *Energy and Buildings* 33 (4): 319–331.

DesignBuilder. 2016. *DesignBuilder Documentation, Design Builder User Manual Version 5*. UK: DesignBuilder Software Ltd.

Ekici, Berk, Cemre Cubukcuoglu, Michela Turrin, and I. Sevil Sariyildiz. 2019. "Performative Computational Architecture Using Swarm and Evolutionary Optimisation: A Review." *Building and Environment* 147 (January): 356–371. doi:10.1016/j.buildenv.2018.10.023.

Ellingwood, Bruce R. 2005. "Risk-Informed Condition Assessment of Civil Infrastructure: State of Practice and Research Issues." *Structure and Infrastructure Engineering* 1 (1): 7–18.

Ellingwood, Bruce R., and Ji Yun Lee. 2016. "Life Cycle Performance Goals for Civil Infrastructure: Intergenerational Risk-Informed Decisions." *Structure and Infrastructure Engineering* 12 (7): 822–829.

Ellingwood, Bruce R., and Paulos Beraki Tekie. 1999. "Wind Load Statistics for Probability-Based Structural Design." *Journal of Structural Engineering* 125 (4): 453–463.

FEMA. 2012. *FEMA P-58: Seismic Performance Assessment of Buildings. FEMA P-58*. Washington, DC: Building Seismic Safety Council for The Federal Emergency Management Agency.

FEMA, Pacific Disaster Center, and USGS. 2017. *Hazus® Estimated Annualized Earthquake Losses for the United States*. FEMA P-366. Hazus Estimated Annualized Earthquake Losses for the United States, The Federal Emergency Management Agency. Washington, DC.

Ferreira, Rodrigo JP, Adiel Teixeira de Almeida, and Cristiano AV Cavalcante. 2009. "A Multi-Criteria Decision Model to Determine Inspection Intervals of Condition Monitoring Based on Delay Time Analysis." *Reliability Engineering & System Safety* 94 (5): 905–912.

FHWA. 1994. *Technical Advisory: Motor Vehicle Accident Costs. T7570.2*. Washington, DC: Federal Highway Administration), U.S. Dept. of Transportation.

Han, Ruilong, Yue Li, and John van de Lindt. 2016. "Seismic Loss Estimation with Consideration of Aftershock Hazard and Post-Quake Decisions." *ASCE-ASME Journal of Risk and Uncertainty in Engineering Systems, Part A: Civil Engineering* 2 (4): 04016005.

Hopfe, Christina J., Godfried L. M. Augenbroe, and Jan L. M. Hensen. 2013. "Multi-Criteria Decision Making Under Uncertainty in Building Performance Assessment." *Building and Environment* 69 (November): 81–90. doi:10.1016/j.buildenv.2013.07.019.

Ibn-Mohammed, Taofeeq, Rick Greenough, S. Taylor, Leticia Ozawa-Meida, and Adolf Acquaye. 2013. "Operational vs. Embodied Emissions in Buildings—A Review of Current Trends." *Energy and Buildings* 66: 232–245.

Invidiata, Andrea, Monica Lavagna, and Enedir Ghisi. 2018. "Selecting Design Strategies Using Multi-Criteria Decision Making to Improve the Sustainability of Buildings." *Building and Environment* 139 (July): 58–68. doi:10.1016/j.buildenv.2018.04.041.

Jafari, Amirhosein, and Vanessa Valentin. 2018. "Selection of Optimization Objectives for Decision-Making in Building Energy Retrofits." *Building and Environment* 130 (February): 94–103. doi:10.1016/j.buildenv.2017.12.027.

Junnila, Seppo, Arpad Horvath, and Angela Acree Guggemos. 2006. "Life-Cycle Assessment of Office Buildings in Europe and the United States." *Journal of Infrastructure Systems* 12 (1): 10–17.

Kamali, Mohammad, Kasun Hewage, and Abbas S. Milani. 2018. "Life Cycle Sustainability Performance Assessment Framework for Residential Modular Buildings: Aggregated Sustainability Indices." *Building and Environment* 138 (June): 21–41. doi:10.1016/j.buildenv.2018.04.019.

Kneifel, Joshua. 2010. "Life-Cycle Carbon and Cost Analysis of Energy Efficiency Measures in New Commercial Buildings." *Energy and Buildings* 42 (3): 333–340.

Kokaraki, Nikoleta, Christina J. Hopfe, Elaine Robinson, and Elli Nikolaidou. 2019. "Testing the Reliability of Deterministic Multi-Criteria Decision-Making Methods Using Building Performance Simulation." *Renewable and Sustainable Energy Reviews* 112: 991–1007.

Kolozvari, Kristijan, Kutay Orakcal, and John W. Wallace. 2014. "Modeling of Cyclic Shear-Flexure Interaction in Reinforced

Concrete Structural Walls. I: Theory." *Journal of Structural Engineering* 141 (5): 04014135.

Lavappa, Priya D., and Joshua D. Kneifel. 2018. *NISTIR 85-3273-33: Energy Price Indices and Discount Factors for Life-Cycle Cost Analysis – 2018, Annual Supplement to NIST Handbook 135*. US Department of Commerce, National Institute of Standards and Technology. doi:10.6028/NIST.IR.85-3273-33.

Lee, Ji Yun, Henry V. Burton, and David Lallemant. 2018. "Adaptive Decision-Making for Civil Infrastructure Systems and Communities Exposed to Evolving Risks." *Structural Safety* 75: 1–12.

Lloyd, Shannon M., and Robert Ries. 2007. "Characterizing, Propagating, and Analyzing Uncertainty in Life-Cycle Assessment: A Survey of Quantitative Approaches." *Journal of Industrial Ecology* 11 (1): 161–179. doi:10.1162/jiec.2007.1136.

Martínez-Rocamora, Alejandro, Jaime Solís-Guzmán, and Madelyn Marrero. 2017. "Ecological Footprint of the Use and Maintenance Phase of Buildings: Maintenance Tasks and Final Results." *Energy and Buildings* 155 (November): 339–351. doi:10.1016/j.enbuild.2017.09.038.

Mazzoni, Silvia, Frank McKenna, Michael H. Scott, and Gregory L. Fenves. 2006. "The Open System for Earthquake Engineering Simulation (OpenSEES) User Command-Language Manual.".

Mitrani-Reiser, Judith. 2007. *An Ounce of Prevention: Probabilistic Loss Estimation for Performance-Based Earthquake Engineering*. Pasadena, CA: California Institute of Technology.

Nadoushani, Moussavi, S. Zahra, Ali Akbarnezhad, Javier Ferre Jornet, and Jianzhuang Xiao. 2017. "Multi-Criteria Selection of Façade Systems Based on Sustainability Criteria." *Building and Environment* 121 (August): 67–78. doi:10.1016/j.buildenv.2017.05.016.

Ochoa, Luis, Chris Hendrickson, and H. Scott Matthews. 2002. "Economic Input-Output Life-Cycle Assessment of US Residential Buildings." *Journal of Infrastructure Systems* 8 (4): 132–138.

Padgett, Jamie Ellen, and Reginald DesRoches. 2007. "Sensitivity of Seismic Response and Fragility to Parameter Uncertainty." *Journal of Structural Engineering* 133 (12): 1710–1718.

Padgett, Jamie E., and Yue Li. 2016. "Risk-Based Assessment of Sustainability and Hazard Resistance of Structural Design." *Journal of Performance of Constructed Facilities* 30: 2.

Park, Hyo Seon, Jin Woo Hwang, and Byung Kwan Oh. 2018. "Integrated Analysis Model for Assessing CO2 Emissions, Seismic Performance, and Costs of Buildings Through Performance-Based Optimal Seismic Design with Sustainability." *Energy and Buildings* 158 (January): 761–775. doi:10.1016/j.enbuild.2017.10.070.

Ramirez, C.Marcelo, and Eduardo Miranda. 2012. "Significance of Residual Drifts in Building Earthquake Loss Estimation." *Earthquake Engineering & Structural Dynamics* 41: 1477–1493. doi:10.1002/eqe.

Ramon, Jose, and San Cristobal. 2012. *Multi Criteria Analysis in the Renewable Energy Industry*. Springer-Verlag London. doi:10.1007/978-1-4471-2346-0.

Robati, Mehdi, Georgios Kokogiannakis, and Timothy J. McCarthy. 2017. "Impact of Structural Design Solutions on the Energy and Thermal Performance of an Australian Office Building." *Building and Environment* 124: 258–282.

Roostaie, S., N. Nawari, and C. J. Kibert. 2019. ""Sustainability and Resilience: A Review of Definitions, Relationships, and Their Integration Into a Combined Building Assessment Framework." *Building and Environment*, doi:10.1016/j.buildenv.2019.02.042.

RSMeans. 2018. *RSMeans Data Online*. Rockland, MA: Gordian Rsmeans. com.

Sutley, Elaina J., John W. van de Lindt, and Lori Peek. 2016. "Community-Level Framework for Seismic Resilience. II: Multiobjective Optimization and Illustrative Examples." *Natural Hazards Review* 18 (3): 04016015.

Tran, Thien A., and John W. Wallace. 2015. "Cyclic Testing of Moderate-Aspect-Ratio Reinforced Concrete Structural Walls." *ACI Structural Journal* 112 (6): 653.

Triantaphyllou, Evangelos, B. Shu, S. Nieto Sanchez, and Tony Ray. 1998. "Multi-Criteria Decision Making: An Operations Research Approach." *Encyclopedia of Electrical and Electronics Engineering* 15: 175–186.

US BLS. 2018. "Average Energy Prices In Boston-Cambridge-Newton – December 2018 : New England Information Office : U.S. Bureau of Labor Statistics." https://www.bls.gov/regions/new-england/news-release/averageenergyprices_boston.htm.

Wallenius, Jyrki, James S. Dyer, Peter C. Fishburn, Ralph E. Steuer, Stanley Zionts, and Kalyanmoy Deb. 2008. "Multiple Criteria Decision Making, Multiattribute Utility Theory: Recent Accomplishments and What Lies Ahead." *Management Science* 54 (7): 1336–1349.

Wang, Jiangyu, Huanxin Chen, Yue Yuan, and Yao Huang. 2019. "A Novel Efficient Optimization Algorithm for Parameter Estimation of Building Thermal Dynamic Models." *Building and Environment* 153 (April): 233–240. doi:10.1016/j.buildenv.2019.02.006.

Wood, David A., and Rassoul Khosravanian. 2015. "Exponential Utility Functions Aid Upstream Decision Making." *Journal of Natural Gas Science and Engineering* 27: 1482–1494.

Zavadskas, Edmundas Kazimieras, Artūras Kaklauskas, Friedel Peldschus, and Zenonas Turskis. 2007. "Multi-Attribute Assessment of Road Design Solutions by Using the COPRAS Method." *Baltic Journal of Road & Bridge Engineering* 2: 4.

Zheng, Linzi, and Joseph Lai. 2018. "Environmental and Economic Evaluations of Building Energy Retrofits: Case Study of a Commercial Building." *Building and Environment* 145 (November): 14–23. doi:10.1016/j.buildenv.2018.09.007.